LBNL NUMBER TBD

ERNEST ORLANDO LAWRENCE
BERKELEY NATIONAL LABORATORY

Inter-laboratory comparison using integrating sphere spectrophotometers to measure reflectance and transmittance of specular, diffuse, and light-redirecting glazing products

Jacob C. Jonsson and Charlie Curcija

ENVIRONMENTAL ENERGY
TECHNOLOGIES DIVISION

SEPTEMBER 14, 2012

Abstract

An inter-laboratory comparison (ILC) between glazing manufacturers that submit data to the International Glazing Database (IGDB) is carried out every four years. This time a large number of independent laboratories were included in addition to the IGBD submitters, in total over 50 boxes of samples were sent out in parallel.

Each box contained 5 specular samples, consisting of clear float glass, low-e coated glass, laminates, and an applied film on clear glass. New for the IGDB submitters were 5 diffuse samples, 2 fritted glass samples, a diffuse laminate, a light-redirecting daylighting film, and a shade fabric with an inhomogeneous pattern.

The samples were characterized by each participant in the solar optical range, 300 nm - 2500 nm, as well as the thermal infrared from $5\mu m$–$25\mu m$. Spectral data was inspected for anomalies such as systematic absorption and non-continuous steps due to instrument design and operation.

Spectral averaged data was calculated and used to compare the results from the different laboratories. Such comparisons indicated that use of a diffuse reference for specular measurements marginally increased the measured result. For diffuse products the effects of sphere geometry and design influenced the results to a significant degree.

1 Introduction

The International Glazings Database (IGDB)[1] contains data of glazing materials for all the glass used in windows that are sold in the US. Lawrence Berkeley National Laboratory (LBNL) maintains the database on commission of the National Fenestration Rating Council (NFRC).

With over 4000 entries in 2012 and increasing with hundreds of new entries every quarter it is not possible for LBNL to measure all the glass. Instead manufacturers measure (or use certified test labs) and submit data which is peer-reviewed by all submitters and other interested parties. To be allowed to submit laboratories have to participate in an inter-laboratory comparison (ILC) every four years and upon joining. This is a procedure that allow both contributors and database maintainers to confirm that the measurement capabilities of the laboratories are of high quality.

The IGDB contains optical information in the wavelength region between 300-2500 nm where transmittance as well as reflectance for both the front and the back surface is recorded at normal angle of incidence. In addition to that emissivity, obtained through measurement of reflectance between 5 and 25 μm, is recorded for both the front and back surface.

The goal for submitters is to pass within the tolerances dictated by NFRC document 302[2] which states that transmittances should be within 1% and reflectance/emissivity withing 2%. As an organizing entity LBNL aims to educate and help submitters troubleshoot any issues that give rise to systematic errors.

LBNL also provides tools for accessing the data in the database. The WINDOW [3] tool that is used to calculated the properties of a window composed of one or more glazings and the frame was expanded to allow calculation of scattering layers for which BSDF (bi-directional scattering distribution function[1]. With this new capability manufacturers of fritted glass, diffuse laminates, Venetian blinds, shade screens, and light-redirecting products wanted to submit their products to the IGDB as well. Instead of that happening a new database was started, the Complex Glazing Database (CGDB), which is designed to handle all glazing products that cannot be accurately described by the limited properties stored in the IGDB. Not only light scattering products, but also dynamic glazings such as thermochromics and electrochromics are allowed.

Measurement of scattering samples has been studied in the past with focus on specific aspects of the instrument and/or material[4, 5, 6, 7, 8, 9, 10, 11, 12, 13, 14, 15, 16, 17, 18, 19] and also on ILC level[20, 21, 22, 23, 24]. Based on that research it was of interest to quantify the variation between participants just measuring as they always do without instrument and sample dependent corrections. For this reason light-scattering samples were for the first time included in the ILC to quantify the variation seen and to find out if the procedure for specular samples was viable for diffuse samples as well.

The ILC is a *living* ILC and does not necessarily contain the first result submitted by a

[1] BRDF and BTDF are commonly used to describe reflectance and scattering, the term BSDF is used to indicate both properties together.

participant and it also allows participants to join over time (to avoid them having to wait for the next one to be allowed to submit data to the IGDB). As errors are found submitters are encouraged to correct procedures or update equipment so that they are allowed to submit data to the IGDB. The risk of this practice is that if any of the recommended solutions introduces new systematic errors this will start to influence the average. Therefore this report tries to highlight the recommendations made so that they can be challenged.

2 Samples

The ILC was a parallel ILC, i.e. all participants get their own set of samples. In addition to speed gain compared to a serial ILC where a single set of samples is passed around this has also proven valuable in the past for the participants since they can go back and remeasure their samples after moving or modifying their measurement equipment.

2.1 Selection committee

Mike Rubin, previously employed at LBNL, organized a sample selection committee consisting of Dave Haskins, PPG; Jordan Lagerman, Cardinal; Jason Theios, Guardian; Bob Curtin, AGC; Dave Duly, NSG; Dan Wacek, Viracon; Raghu Padiyath, 3M; Jacob C. Jonsson, LBNL; Brija Nand, Southwall; Julia Schimmelpenningh, Solutia.

2.2 Specular sample selection

A total of five samples were selected from three companies, PPG, Solutia, and 3M. PPG produced a clear low-iron glass and also clear low-iron glass coated with a low-e coating. All glass used in the ILC was taken from the same production run. Solutia created laminates using the uncoated and coated samples. 3M applied a reflecting film to to the clear substrate for the final sample. To summarize:

1. 6 mm Starphire, PPG
2. 6 mm Starphire coated with triple silver Solarban 70XL, PPG
3. 2 pieces of product 1 laminated with Solutia Saflex 0.76 mm R series PVB, PPG and Solutia
4. Product 1 and product 2 laminated with Solutia Saflex 0.76 mm R series PVB, PPG and Solutia
5. Product 1 with applied film, PPG and 3M

A total of 50 boxes were sent out in the initial round, another 50 were kept at LBNL to allow for future inclusion of laboratories to submit to the IGDB.

2.3 Scattering sample selection

A total of five samples were selected from three companies, Viracon, Solutia, Ferrari, and 3M. Viracon provided two samples, a clear unpigmented fritted glass and one with white pigments. Both fritted glass samples were on 6 mm Starphire low-iron glass form PPG. Solutia provided a white inter-layer laminate on 3 mm Starphire glass. 3M provided a light-redirecting applied film on 6 mm Starphire. Ferrari provided a PVC over PET shade fabric with irregular openness.

7. Viracon V1086 simulated sandblasted on 6 mm Starphire
8. Viracon V175 white on 6 mm Starphire
9. Solutia diffuse inter-layer on 3 mm Starphire
10. 3M light-redirecting applied film on 6 mm Starphire
11. PVC over PET shade screen from Ferrari Textiles Corporation Soltis 93 - 3002 sand

2.4 Sample variation

Transmittance measurements of each sample was carried out at 550 nm to give an indication of the sample variation, this was done at LBNL before samples were shipped out. The transmittance was measured for 20 seconds with the signal sampled every second, typical variation in reading over 20 seconds was ± 0.0002. The difference between samples and the average was calculated by subtracting the mean from each measured value. The extreme values as well as two times the standard deviation is shown in figure 1.

The variation of the clear glass samples and the clear clear laminates was very small. All in all, more than 90% of the samples were within 0.005 absolute difference from the mean value. The outliers among the low-e coatings is believed to be due to defects in the form of scratches from shipping and handling the samples. The conclusion from looking at this data is that it is of little benefit to force the manufacturers to measure more than one sample.

The variation among the scattering samples was considerably larger. The fritted glass samples were prepared at the sample size by hand rather than the industrial process for panes. This is one reason why the sample variation is greater for those sample. Variation over a single specimen was within ± 0.002 for sample 6 so orientation and positioning is not an issue.

After the variation had been measured at LBNL, the samples where packaged, shipped, and upon reception cleaned by the recipient before they measured it with their instrument. Typical cleaning procedures consisted of soap and (deionized) water, rinsing in ethanol and drying with compressed air or nitrogen.

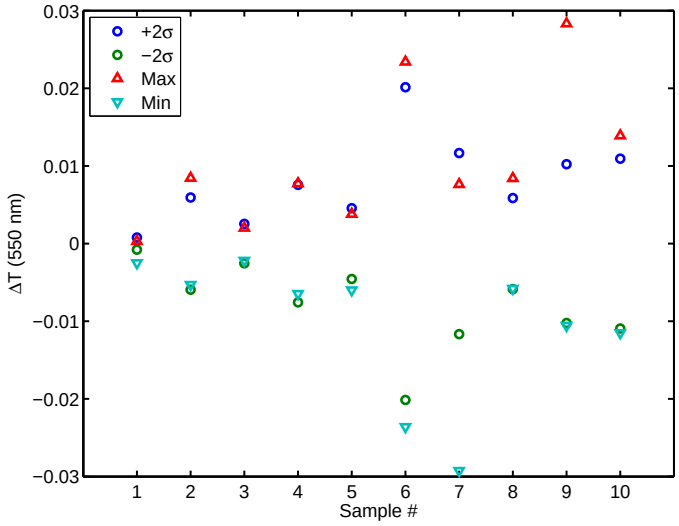

Figure 1: The absolute variation of transmittance measured at 550 nm for the ten different samples.

3 Solar optical range, 300–2500 nm

3.1 Instruments and detectors used

A majority of the ILC participants used Perkin-Elmer Lambda 900/950 instruments fitted with a 150 mm integrating sphere. The low number of other instrument types limits the ability to draw conclusions from the results. A breakdown is shown in figure 2a).

The typical detector combination is a photo multiplier tube (PMT) for the visible range and a lead sulfide (PbS) detector for the NIR. The Lambda 1050 instruments feature an indium gallium arsenide (InGaAs) detector instead. All participants had an integrating sphere, the diameter distribution is shown in figure 2b).

With such a dominance of a few detector systems and instruments it is impossible to confidently say that the other instruments and detectors are performing better or worse. No error was tied to a single brand or detector type.

3.2 Specular samples

Over 40 sets of data were collected for the specular sample set. Some of these had errors in them that were detected early which allowed the participant to resubmit remeasured data.

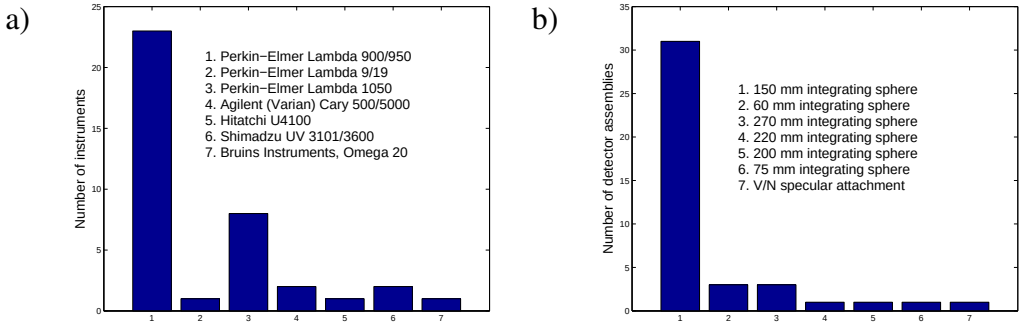

Figure 2: a) Distribution of instruments among the participants. b) Distribution of detector systems used.

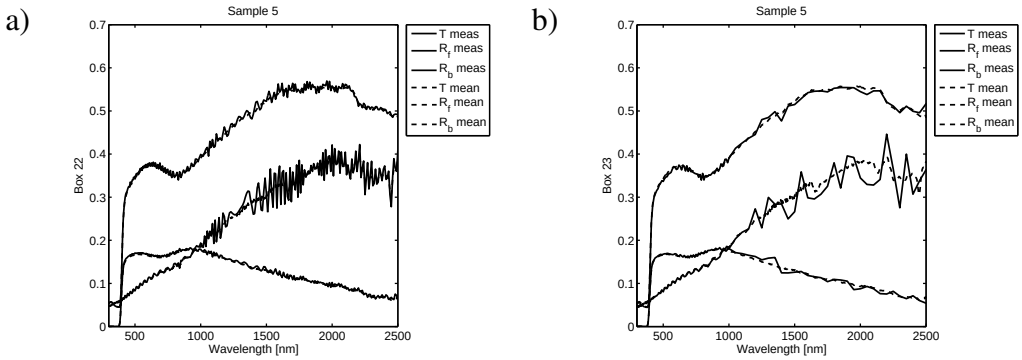

Figure 3: Data for the applied film sample. a) Data presented with 5 nm steps. b) Data presented with 50 nm steps.

3.2.1 Effects of large wavelength steps when measuring applied films

IGDB has in the past required steps of 50 nm or shorter for data at wavelengths longer than 1000 nm. The consequences of using the longest step length is shown in figure 3b); with very narrow interference fringes it is more or less random what value is reported in the range from high to low.

There are two ways to avoid this, the practical way is to measure at shorter steps, as shown in figure 3a), which makes it less probable that streaks of high or low values will skew the integrated values.

The second way is to adjust the bandwidth of light used to illuminate the sample. The grating of a spectrophotometer in practice produces a distribution of wavelengths and the bandwidth of this is controlled by a slit in the optical system. This will create an average over multiple wavelengths which creates a smoother curve. While not an accurate representation of the interference fringes it will produce accurate results for integrated values.

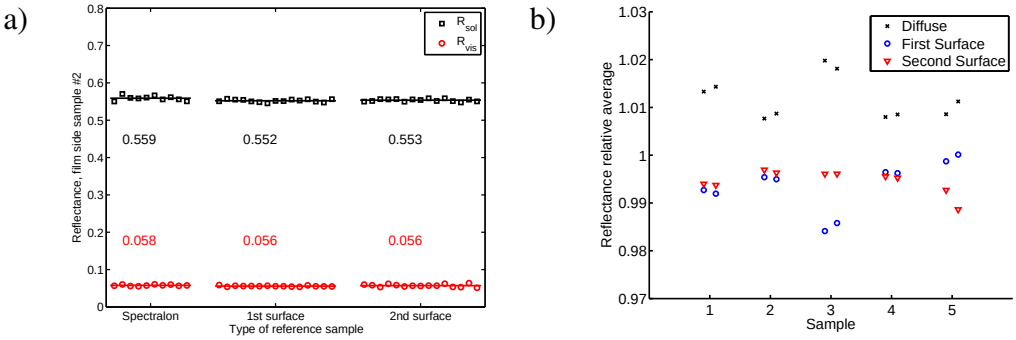

Figure 4: Integrated reflectance grouped for kind of reference sample. The average value for each group is written next to the curve. The diffuse Spectralon group has a slightly higher average than the other two. a) Film-side reflectance of sample #2 showing the individual measurements for each participant. b) Showing the reflectance relative the average for that sample for all measured reflectances. The two values for each sample is front and back reflectance.

3.2.2 Diffuse versus specular reference

Integrating sphere theory suggests that using a diffuse reference sample of the same material as the sphere wall will give you an absolute reflectance measurement for specular samples. This requires that the detector response is identical for light incident on the specular port and the reflectance sample position. Since commercial integrating spheres are not ideal spheres it is not obvious that it would give the same result as when using a specular reference mirror. Data from this ILC can be used to compare results using diffuse standards, first surface mirrors, and second surface mirrors.

The specular mirrors have been divided between first, or front, surface mirrors and second surface mirrors. For the first surface mirrors the mirror film is exposed to air and will be in direct contact with the instrument. Even though some of these mirrors are protected with a surface coating they are sensitive to scratching which can occur when mounting against the sphere wall. The second surface mirrors have the mirror film sealed on the back of a transparent substrate. This protection results in a slightly lower reflectance but makes the mirror less sensible to degradation.

The reflectance measured is graphed versus the type of reference used in figure 4. The metal coating of sample #2 is shown in figure 4a) and the solar reflectance is slightly higher, about .005 or 1% relative, on average but the visible reflectance is seemingly independent of reference sample. In figure 4b) the average of each group is graphed divided by the average for all groups. It shows that for all 10 measured reflectances, counting front and back of the five samples, the data submitted using a Spectralon reference is consistently higher than average and the specular mirrors are lower.

One way to get a value that is too high is if the reference sample has a lower reflectance than it is supposed to. In the case of a specular reference mirror that happens if the surface

has a lower reflectance than its certificate. In the case of a diffuse reference sample it happens if the Spectralon reference has a lower reflectance than the specular port. By lower reflectance in this case it is not only necessary to consider the actual reflectance of the material but also the response from the detector in the integrating sphere. So the sphere geometry coupled with the scattering distribution of the material, both the reference and the specular port, could play a role in any deviation from the true value. Studies have been made on the variation in detector response with respect to where in the sphere the light is coming from [11, 25]. This variation largely is due to the spehere design and the deviation from an ideal sphere by insertion of baffles and ports for various experimental purposes.

It has been shown that Spectralon reflectance decreases with time even if the material is kept in the dark[26]. One possible hypothesis is that the Spectralon reference deteriorates faster than the specular port due to handling and that this gives rise to a systematically too high measured reflectance.

Another possibility is that the detector response is different for light scattered from the specular port and the sample port. The largest contribution would be the entrance port which is close to the normal in the case of the reference measurement but not in direct field of view from were the specular port.

The loss through the entrance port for the diffuse reference can be obtained by integrating the BRDF of the reference over the solid angle of the entrance port. The calculation can be simplified by setting the exit angle to 0 degrees rather than the near normal of most instruments. In the case of constant BRDF the equation can be simplified as

$$\text{Loss} = \int \text{BRDF} \cos\theta d\Omega = 2\pi \cdot \text{BSDF} \left(\frac{\cos^2 \theta_{lo}}{2} - \frac{\cos^2 \theta_{hi}}{2}) \right), \tag{1}$$

where θ_{lo} is zero for normal angle of incidence and θ_{hi} is obtained from the sphere geometry as

$$\theta = \text{atan}(\frac{d/2}{D}), \tag{2}$$

where d is the port diameter and D the sphere diameter.

For the most common sphere configurations, 150 mm sphere with port diameters of 19 mm and 25 mm, the correction Loss becomes $.004$ and $.007$, respectively. This can be applied as a relative correction factor to the final result. Applying this correction reduces the difference between the results of diffuse and specular measurements but does not explain the full difference between the two.

3.3 Example of corrected results

This section highlights some of the more confounding problems that show up repeatedly but can be hard to replicate on different instruments.

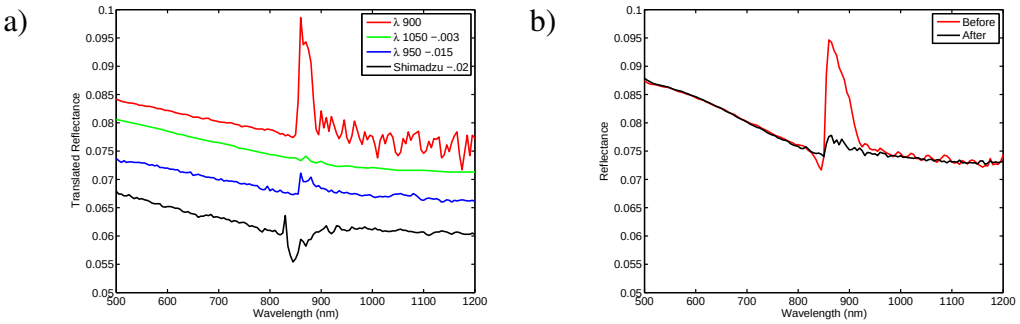

Figure 5: a) Example of different glass reflectance measurement of sample #1, values have been shifted laterally to clearer show the discontinuities. b) Example from a measurement in the ILC conducted in 2007.

3.3.1 Discontinuity at grating change

These spectrophotometers are built to cover two wavelength ranges and mechanical alignment of detectors, gratings, and light sources is an engineering problem that is part of the challenge of building these instruments.

Example of a couple of different instrument results are shown in figure 5a) A step of .02 indicates that you have no room for sample variation if you want to stay within .02 tolerance. Smaller steps are unsightly and could create problems for calculation of optical constants or when deconstructing an applied film or a laminate.

The step shown in figure 5b) was reduced by using a fixed slit width in NIR rather than the default servo setting. It also mattered what the ratio of slit width between the two gratings, best results were obtained when the ratio matched the ratio between the number of grooves per mm for the gratings. This keeps the light spot the same size.

The gratings also have a strong polarizing effect, if the instrument is not fitted with a depolarizer and the sample is polarized there is a possibility that there will be a discontinuity here as well.

3.3.2 Absorption artifacts in NIR

Sample #2 has an exposed metal coating that is highly reflective in NIR. The flat shape of the reflectance for the coated side makes it easy to spot any absorption artifacts in that range. An example of the effect is shown in figure 6 from a metal coated sample used in the ILC 2007, sample #2 in this ILC has similar properties but very few submissions showed this effect so far this year which is why it is exemplified using data from 2007.

It is hard to repeat this effect but a theory for how this happens is suggested. The submissions in figure 6 all used a diffuse reference and a Spectralon integrating sphere. In theory this should give the reflectance value assuming the detector response is the same for light incident on the reference sample and the specular port[2]. These two sphere locations

[2]It is common, but not necessary that an integrating sphere has a specular port, if none is present it is the

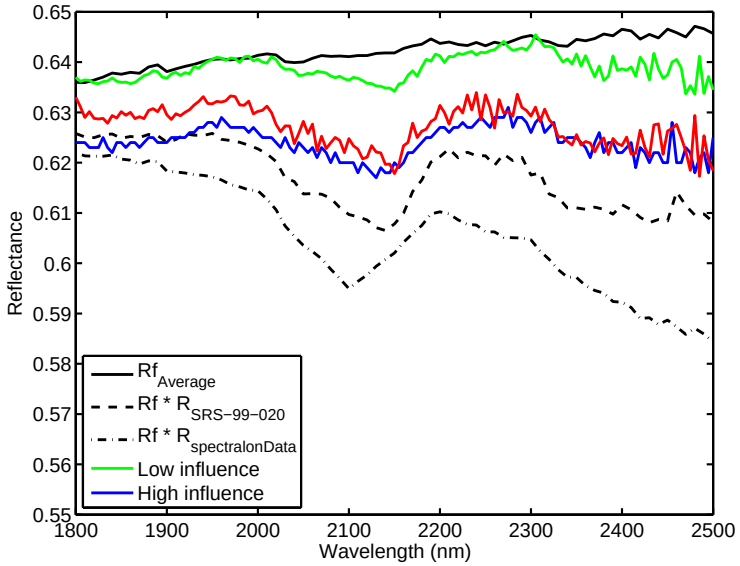

Figure 6: Average reflectance of a metal coated glass substrate and that value multiplied with the reflectance of Spectralon contrasted against submissions with absorption artifacts.

are both baffled and not directly in the detector field of view and in those cases the most plausible explanation would be that the reference and the port have degraded differently. Some submitters tried to clean their reference samples but without any improvement. The only way they could get accurate results was to use a specular reference mirror.

3.4 Diffuse and light-scattering samples

Since the complex part of the ILC was not mandatory for the IGDB submitters there were fewer submission, but still over 15 sets of data was reported in a useful format.

Sample 8, the diffuse laminate, has been left out of the discussion, the fritted glass samples cover the issues for that sample in a clearer way and in addition those samples have issues regarding front and back issues.

3.4.1 Transmittance of thick scattering samples

A thickness of 6 mm is common for fritted glass and diffuse laminates so these samples are not extreme products that are not representative for the products that need to be measured.

The measured spectra from samples 6 and 7 are shown in figure 7a) and b), respectively. The spread is significantly larger than for the specular samples. Two instruments,

sphere wall at the spot where the specular reflection first interacts with the sphere that has to have the same detector response as the reference sample

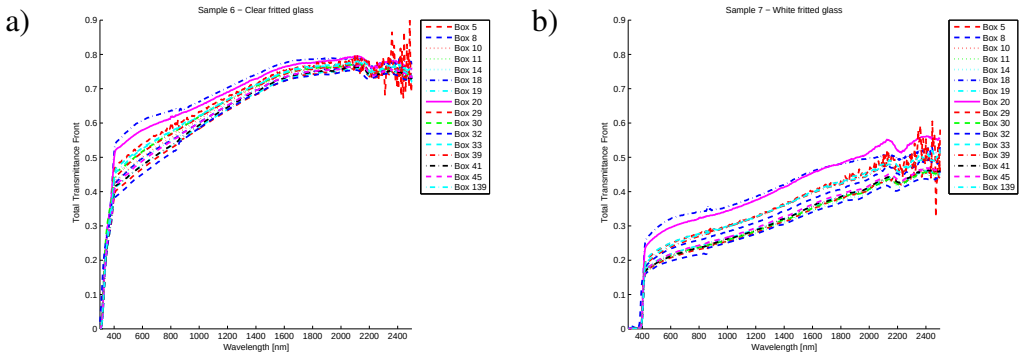

Figure 7: Measured transmittance of the clear fritted glass in a) and the white fritted glass in b). Box 18 and box 20 have integrating spheres that are larger than the others and those obtain significantly larger results. For the samples with more similar sphere size the range is still around ± 0.03.

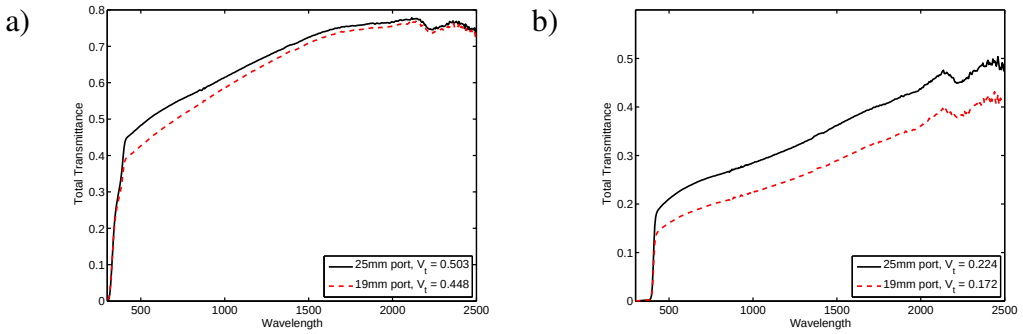

Figure 8: Total transmittance versus wavelength for a) sample 6 and b) sample 7. As the port is made smaller, a larger fraction of the scattered light misses it and fails to contribute to the signal.

box 18 and 20, report significantly larger values than the main group of results, but even in the main group the variation is significantly larger than for specular samples.

There is a strong correlation between the ratio of beam size to port radius and low measured transmittance, a majority of the instruments are 150 mm spheres with a port diameter of either 19 mm or 25 mm. The beam size at the entrance port varies more, partially because it is a hard value to measure accurately. Box 20 has a 38 mm entrance port and box 18 is measured using a 270 mm integrating sphere with a 50 mm entrance port, but the beam area is close to the other 150 mm spheres. That sample thickness, port size, and beam size combine to give a measured value that is different from the actual transmittance has been studied in theory[20, 17].

In practice figure 8 shows what happens when only the port size is changed and everything else kept constant. It is intuitive that a smaller aperture will block more of the high angle scattering light and hence give a lower measured result. The large variation

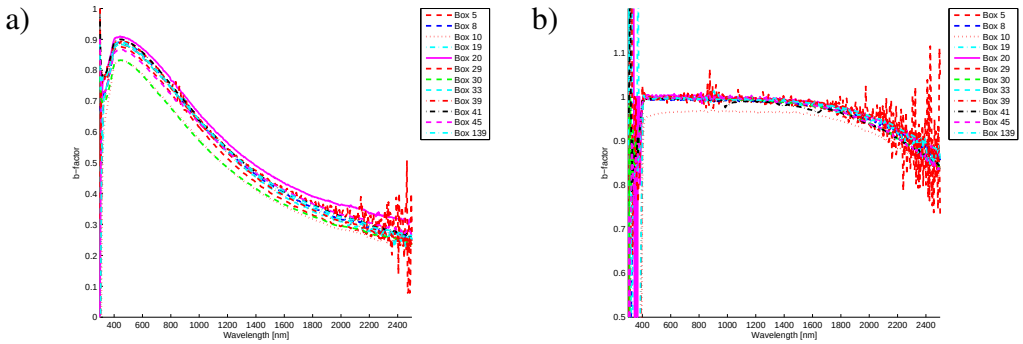

Figure 9: Diffuse transmittance divided by total transmittance versus wavelength for a) sample 6 and b) sample 7. The agreement is better the more scattering the sample is, which can be seen comparing shorter and longer wavelengths for sample 6.

between instruments in beam size and port size makes it hard but not impossible to make corrections. However, since the sample thickness and scattering distribution also influence the result such an instrument only correction would not suffice to give accurate results.

3.4.2 Diffuseness of thick scattering samples

Scattered and specular can give different detector response as was discussed in section 3.2.2. Most commercial integrating spheres that can be used for both reflectance and transmittance allows for measuring the diffuse only transmittance in addition to the total transmittance. The ratio of diffuse component to total is often used to quantify the haze of the sample[27]. The ratio is also called *b-factor* in the context of correcting the specular component differently from the diffuse with regards to reference reflectance [28].

The variation of measured diffuse to total ratio is shown in figure 9. There is a clear wavelength dependence of the scattering both for the clear frit in figure 9a) and the white frit in figure 9b).

The ranking of the participants follow that of total transmittance where smaller ports and larger beam to port ratio gets lower results. This is supports the idea that the high-angle scattering is the part that gets lost and not the specular component. Consider

$$b_{measured} = \frac{T^{diff}_{measured}}{T^{tot}_{measured}} = \frac{T^{diff} - L}{T^{tot} - L}, \tag{3}$$

where L is the faction of light lost not reaching the detector. The larger L is the larger the difference between $b_{measured}$ and the real b is. Since L is sample and instrument dependent there is no obvious solution to get the results to converge.

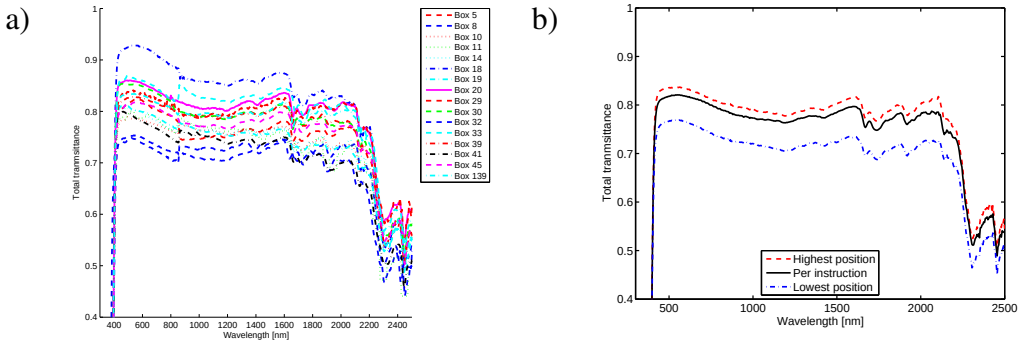

Figure 10: a) Submitted results for transmittance of sample 9. b) The same sample measured with the same instrument at three different rotations.

3.4.3 Transmittance of a light-redirecting sample

Sample 9, an applied film with a refractive light-redirecting micro structure, differs from the other diffuse samples in that the distribution of the light is redirected towards several hot-spots rather than scattering light isotropically. In addition to the major direction there is minor contribution in the whole plane created by the incident beam and the outgoing major direction. The redirection at normal angle of incidence was only about 20 degrees, much less than higher angles which is part of the design of the film, it is more effective at redirecting light from a sun high in the sky than at the horizon.

Ideally this scattering plane should not intersect with parts of the sphere that are not ideal, such as ports, the detector, the baffles and straight into the detectors field of view. Based on this assumptions the participants were instructed to orient the sample in such a way that the transmitted light would interact minimally with the non-ideal parts. This can be done by using the instrument in alignment mode with the light at a single visible wavelength or with white light.

When characterized at LBNL the samples were within ± 0.02 as shown in figure 1. Submitted results shown in figure 10a) are mostly grouped in a range of ± 0.05. There are also significant discontinuities at the detector change for some participants, this could depend on polarization effects of the gratings used to obtain monochromatic light in combination with the orientation of the sample.

Measurement of a single sample using a single instrument was carried out to investigate if this ± 0.05 range could be explained by rotation. The instrument was set to a single wavelength and slowly rotated in 360 degrees to find minimum and maximum recorded values. Full spectral data was obtained at those positions as well as at the position recommended in the instructions and the difference is showing in figure 10b). The range is close to ± 0.04 which is significantly larger than the sample variation seen. This does not necessarily mean that the rotation is the sole component creating the spread between participants. Furthermore the range obtained from rotating the sample does not have to be the same for spheres of different design.

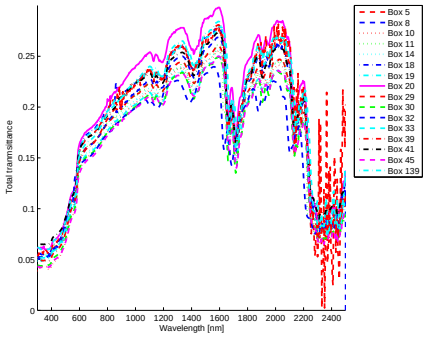

Figure 11: Results from transmittance measurements of sample 10, a thin shade fabric made of PVC over PVB. The large variation agrees to a large extent with the thicker scattering samples.

3.4.4 Transmittance of a thin scattering sample

Sample 10 is a thin sample less than 1 mm in thickness but was perforated with a inhomogeneous pattern of holes. Integrating sphere measurements of shade fabrics have been studied in great detail[29] and even though it is a thin sample the integrating sphere might still give rise to errors. The submitted results are shown in figure 11.

Using white light it was possible to vary the measured transmittance from 0.16 to 0.23 by positioning fewer or more holes under the illuminating beam. This range is sample and instrument dependent. The range will decrease the larger the beam and the more homogeneous the sample is. So while having a small beam results in a beam to port ratio that reduces loss it at the same time increases the probability that holes or fabric will be overrepresented rather than an average.

3.4.5 Reflectance of scattering samples

To a large extent the issues are the same for reflectance of scattering samples as for transmittance. The added complexity is the reflectance of the reference used. However, for a reference with reflectance of 0.98 the relative error is 0.02 which will result in an error of less than 0.01 absolute value for a glazing with a transmittance of around 0.7. This is significantly less than the ± 0.04 ranges seen in measurement but it should still not be neglected, the point is that doing that correction does not solve the majority of the problem.

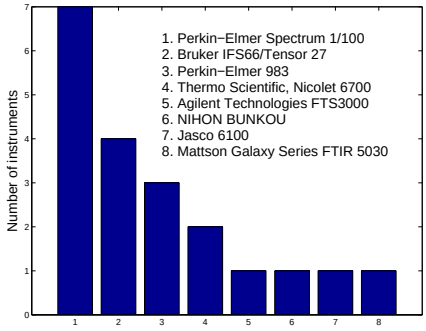

Figure 12: Distribution of instruments used to measure reflectance between $5\mu m$ and $25\mu m$ for calculation of emissivity.

4 Thermal infrared range, 5–25μm

4.1 Instruments used

The IR instrument market is more diverse than the solar optical instrument market and that is seen in the range of instruments used presented in figure 12. The THERMES project[30, 31, 32] did thorough comparisons between dispersive and FTIR instruments and those have not been repeated here since there were only three dispersive instruments in the whole test.

There was a call for submission using emissometer type instruments but only two boxes were measured using those. The results from those two boxes were good but without a larger set of participants it is optimistic to draw any conclusions.

4.2 Emissivity calculations

The IGDB contains information about the emissivity in the infrared range. To obtain this value reflectance is measured and since the samples are opaque in the infrared wavelength region so the absorption is equal to one minus the reflectance. The spectral absorption is weighted using a 300 K black body curve according to NFRC 301[33]. This temperature is the default in the LBNL Optics/Window 6 programs. The IGDB allows submissions where the submitter has calculated the emissivity instead of submitting the measured data.

The calculation of emissivity is not always carried out in this way. The European standard EN673[34] uses a temperature of $283K$ instead of $300K$. A room-temperature blackbody emits about 17% of the total energy at longer wavelengths than $25\mu m$, if the region is extended to $40\mu m$ a different value can be obtained for some materials. The difference in calculated emissivity for low-e coatings is very small though as there is next to no variation in reflectance beyond $25\mu m$. The numerical differences are shown in figure 13 for a single data file from this ILC. The reason to not measure beyond $25\mu m$ is

purely practical in that for a long time it was impossible to purchase a new IR spectrophotometer that could measure longer wavelengths.

The conclusions to draw is that even though the differences are not large it could lead to rounding differently depending on how the emissivity was calculated.

In addition to the choice of black body temperature there is also a transformation from the direct emissivity (which is measured) to the hemispherical emissivity which is the reported property. This is carried out in accordance to NFRC 301[33].

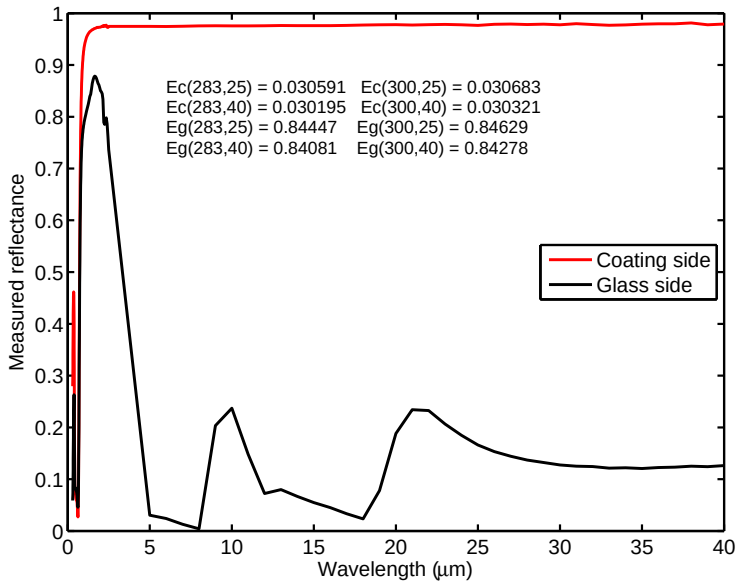

Figure 13: Spectral reflectance measured and hemispherical emissivity calculated for two temperatures, 283 K and 300 K, and using two different upper boundaries for the calculation. The calculation was carried out for both the glass side (E_g-values) and the coated side (E_c-values) of the sample.

4.3 Measurements

Out of the five samples, there were only two surfaces that were not uncoated glass, those were the low-e coating of sample 2 and the applied film of sample 5. By measuring glass emissivity 8 times the laboratories got good information about how the repeatability of the instrument was. An example of such a result is shown in figure 14.

In addition to the glass reflectance the low-e and applied film coatings were both graphed individually. Examples of such measurements are shown in figure 15.

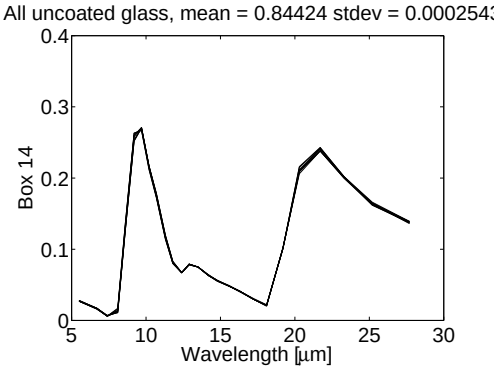

Figure 14: Example of one submitter number 14's reflectance measurement of the 8 uncoated glass surfaces all show together in one graph to demonstrate the instrument variation.

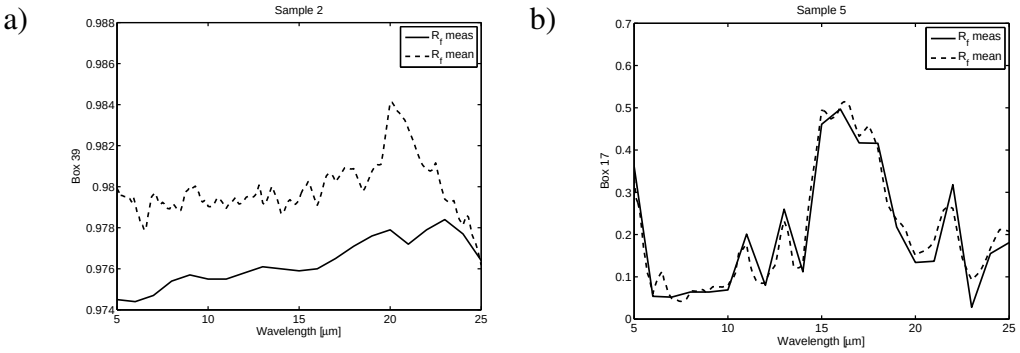

Figure 15: Example of submitted IR reflectance of the low-e coating and the applied film in a) and b), respectively. R_fmeas is the submitter's measured value of the film/coated surface and it is compared to the average of all submitters measured values R_fmean. The index $_f$ indicates film side rather than glass side.

4.4 Calculation of hemispherical emissivity

A two step process is used to calculate the hemispherical emissivity from the near normal IR reflectance measurement measured.

4.4.1 Calculation of normal emissivity

The normal emissivity is calculated by integrating the measured reflectance, $R(\lambda)$, weighted with the black-body emissivity spectrum of a 300 K body, $E_b(\lambda)$, according to

$$\varepsilon_n = \frac{\int_{5\mu m}^{25\mu m}(1 - R(\lambda))E_b(\lambda)\,d\lambda}{\int_{5\mu m}^{25\mu m} E_b(\lambda)\,d\lambda}, \tag{4}$$

where $E_b(\lambda)$ is calculated according to

$$E_b(\lambda) = \frac{C_1}{\lambda^5(\varepsilon^{C_2/\lambda T})}, \tag{5}$$

where the emitted black-body radiation, $E_b(\lambda)$, is given by

C_1 Planck's first constant ($3.743 \times 10^8 W\mu m^4/m^2$)

C_2 Planck's second constant ($1.4387 \times 10^4 mumK$)

T temperature (K)

λ wavelength (μm).

4.4.2 Conversion from normal to hemispherical emissivity

The hemispherical emissivity, rather than the normal emissivity, is the property used in thermal calculations. Rather than to measure the hemispherical value it is calculated using empirical expressions[35].

For uncoated substrates the expression is:

$$\varepsilon_h = 0.1569\varepsilon_n + 3.7669\varepsilon_n^2 - 5.4398\varepsilon_n^3 + 2.47333\varepsilon_n^4 \tag{6}$$

where ε_n is the normal emissivity calculated using equation 4.

For coated substrates the expression is:

$$\varepsilon_h = 1.3217\varepsilon_n - 1.8766\varepsilon_n^2 + 4.6586\varepsilon_n^3 - 5.8349\varepsilon_n^4 + 2.7406\varepsilon^5. \tag{7}$$

4.4.3 Calculated emissivities for samples 1–5

The average value for the low-e coating was 0.024. The average value for the the applied film was 0.77. For the clear glass the average value was 0.84.

5 Conclusions

This report indicates that the state of the participants measurements is in general very healthy, almost all measurements are within the tolerances set by NFRC.

Results shown in sections 3.3.2 and 3.2.2 indicate that a specular reference mirror is preferred compared to a diffuse reference. Since the method of using a Spectralon reference is theoretically sound and works well for some submitters it is still allowed, however, submitters are strongly adviced to switch to using a a calibrated specular mirror instead. This topic has been brought up for discussion in the ASTM E903 committee but not resolved.

Two changes to the IGDB submission procedure are suggested as a result of this ILC and they are both considered to be straight-forward:

1. Switch to require narrower steps that 50 nm in the near infra-red. This is demonstrated in section 3.2.1 on the applied film data. Most instruments already measure this data so it is a small change for submitters.

2. Require emissivity to be submitted as the measured direct IR reflectance. This improves the quality of the database since it allows users to calculate emissivity according the their standard of choice. The submission of self-calculated emissivity data seemed to be the largest problem in section 4. Also, having spectral data uncorrected allows users of the data to perform their own calculations which is useful for as long as there are multiple standard ways of doing these calculations.

It is the intent of LBNL to work with ISO and ASTM standards groups to improve on the language in standards to make it easier for new submitters to find information in the right place on how to carry out good measurements, and if possible prove that the tolerances could be decreased.

For scattering samples it is clear that the result is affected both by the design of the instrument and the scattering properties of the sample. Rigorous control of the beam size and port size would decrease the range of results but still not necessarily give an accurate result. Without a standardized way for operators to carry out sample dependent correction accuracy and precision will be hard to obtain together.

6 Acknowledgment

This work was supported by the Assistant Secretary for Energy Efficiency and Renewable Energy, Building Technologies Program of the U.S. Department of Energy under Contract No. DE-AC02-05CH11231.

All participants contributed significant time in measuring all sample properties and their effort and willingness to work with the authors is greatly appreciated.

Appendix

A List of Participants

An auto-generated list based on the submitters information in the *boxXXinfo.txt* that was included in the submission is show in table 1. The list is not sorted by box number.

Table 1: Autogenerated table from what participant wrote in the *boxnninfo.txt* file. Not listed in box number order.

Institute	**Contact**
3M Company	Raghu Padiyath
AGC Glass Company North America	Bob Curtin
AGC Glass Japan/Asia Pacific	Sigetosi Hirasima
AGC glass Europe	Ingrid Marenne
Arcon Flachglas-Veredlung GmbH & Co.KG	Carsten Ruppe
Belgian Building Research Institute (BBRI)	Gilles Flamant
Berlin Institute of Technology	Stefan Gramm
CEPT, Navrangpura, Ahmedabad.	Dr. Vinod Patel
CSG Holding Co., Ltd.	Chengde Huang
Cardinal Glass Industries	Jordan Lagerman
China Building Material Test & Certification Center)	Wu,Jie
DuPont P&IP Glass Laminating Solutions R&D	Stephanie H. Lott
Erickson Internationa	Mike Martin
Euroglas	Martin Daams
Fraunhofer Institute for Solar Energy Systems	Helen Rose Wilson
Guardian Europe S.a.r.l.	Jos Linden
Guardian Industries Corp	Jason Theios
HanGlas Gunsan R&D Centre	Choi, Junbo
INTERPANE Entwicklungs- und Beratungsesellschaft	Karl Häuser
Lawrence Berkeley National Laboratory	Jacob C. Jonsson
Madico, Inc	Andy Hayes
Madico, Inc., St. Petersburg, FL	John Sandoval
NSG Group	James Farmer

continued on next page

Institute	Contact
Optical Data Associates, LLC	Michael R Jacobson
PFG Building Glass	Rahab Bopape
PPG Industries	Nathaniel Hazelton, Dave Haskins
Pilkington Weiherhammer Laboratory	Dr. Joachim Bretschneider
Shanghai Yaohua Pilkington Glass Co.,LTD	Sun Dahai
Saint-Gobain Glass CRDC	Michel Pichon
Saint-Gobain Solar Gard LLC	Jon Mitchell
Solar Energy Research Institute of Singapore (SERIS)	Teo Wei-Boon, Chen Fangzhi
Solutia Inc.	Julia Schimmelpenningh
Solutia Perforamnce Films	Beth Lawless-Coale
Sonnergy Limited	Michael G Hutchins
Southwall Technologies	Brija Nand
Southwall europe GmbH	Gunnar Spitzer
Stazione Sperimentale del Vetro	Antonio Daneo
The Ångstrom Laboratory, Uppsala University	Arne Roos
Viracon	Dan Wacek
Viridian	Lynton wombwell

B Graphs for all UV/Vis/NIR measurements

The graphs on following pages all show integrated solar and visible optical properties for each sample. The individual markers (squares and circles) show reported values, dotted lines show plus and minus two times the calculated standard deviation for that property, and finally dashed lines show limits imposed by NFRC 302 (.01 for transmittance and .02 for reflectance).

B.1 Sample #1

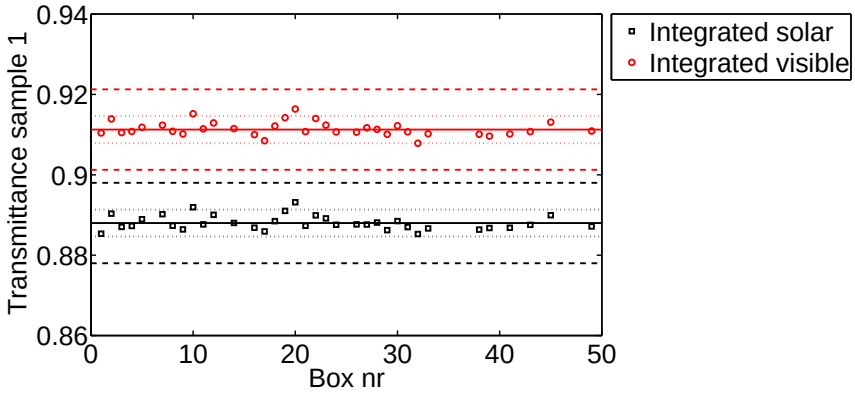
Transmittance sample 1
0.94
0.92
0.9
0.88
0.86
0
10
20
30
40
50
Box nr
Integrated solar
Integrated visible

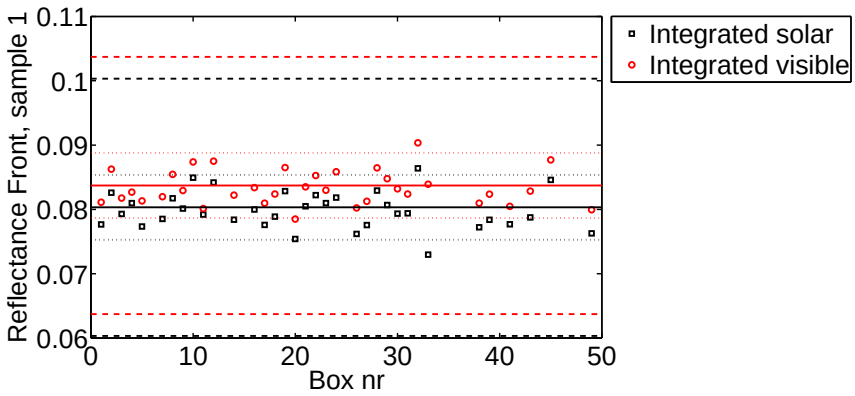
Reflectance Front, sample 1
0.11
0.1
0.09
0.08
0.07
0.06
0
10
20
30
40
50
Box nr
Integrated solar
Integrated visible

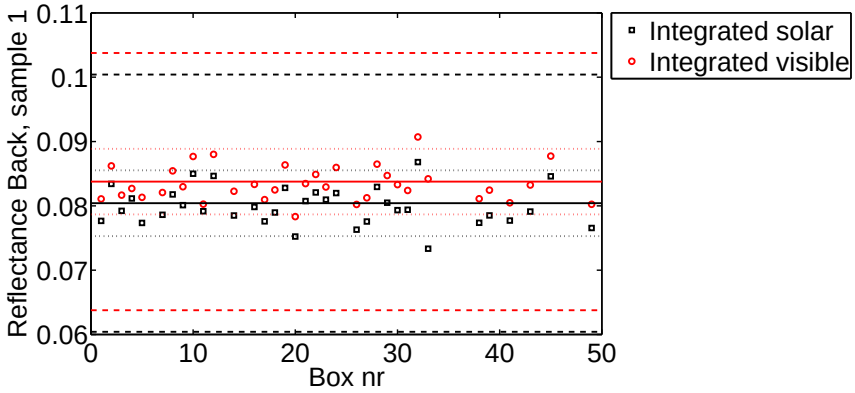
Reflectance Back, sample 1
0.11
0.1
0.09
0.08
0.07
0.06
0
10
20
30
40
50
Box nr
Integrated solar
Integrated visible

B.2 Sample #2

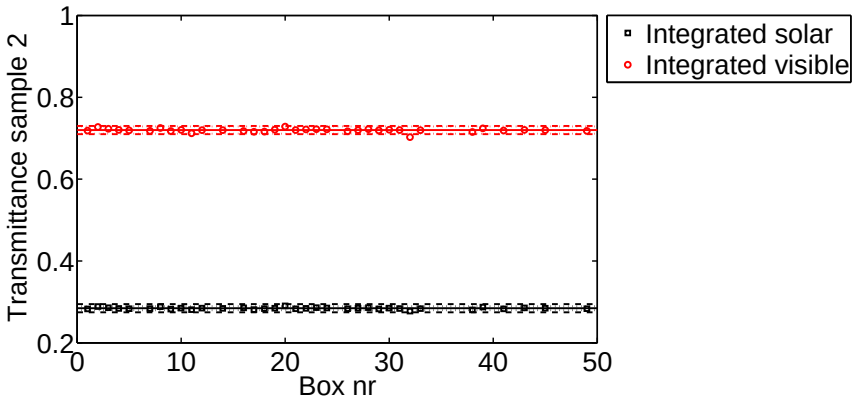
Transmittance sample 2
Box nr
Integrated solar
Integrated visible
0.2
0.4
0.6
0.8
1
0
10
20
30
40
50

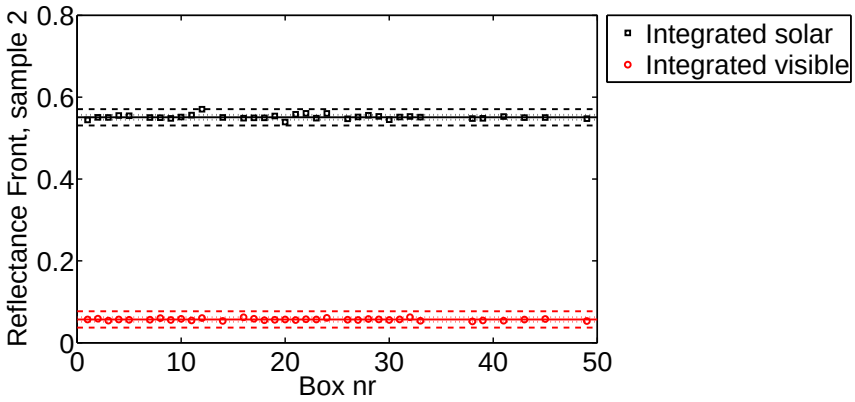
Reflectance Front, sample 2
Box nr
Integrated solar
Integrated visible
0
0.2
0.4
0.6
0.8
0
10
20
30
40
50

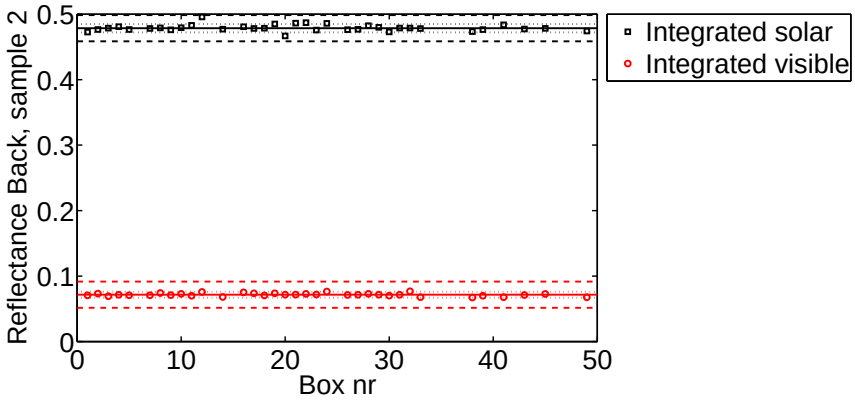
Reflectance Back, sample 2
Box nr
Integrated solar
Integrated visible
0
0.1
0.2
0.3
0.4
0.5
0
10
20
30
40
50

B.3 Sample #3

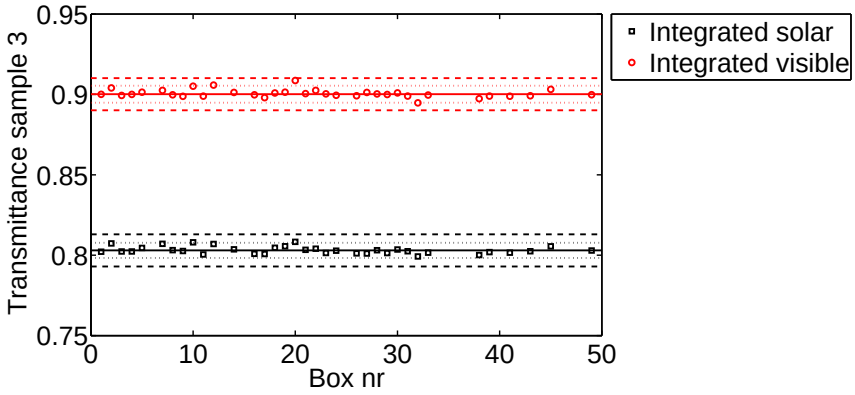
Transmittance sample 3
0.95
0.9
0.85
0.8
0.75
0
10
20
30
40
50
Box nr
Integrated solar
Integrated visible

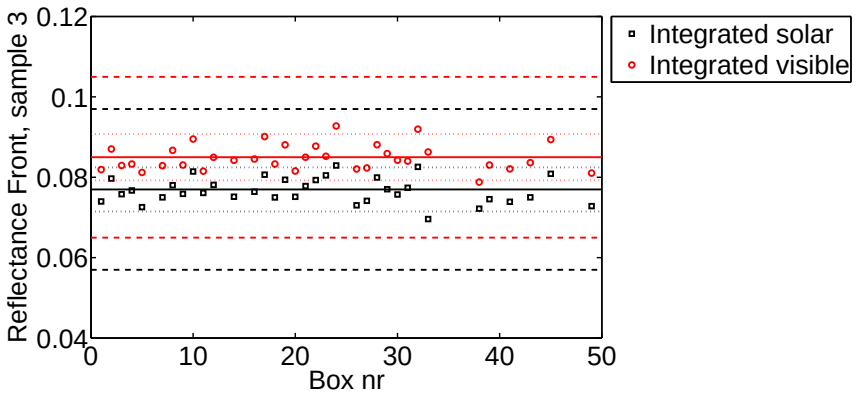
Reflectance Front, sample 3
0.12
0.1
0.08
0.06
0.04
0
10
20
30
40
50
Box nr
Integrated solar
Integrated visible

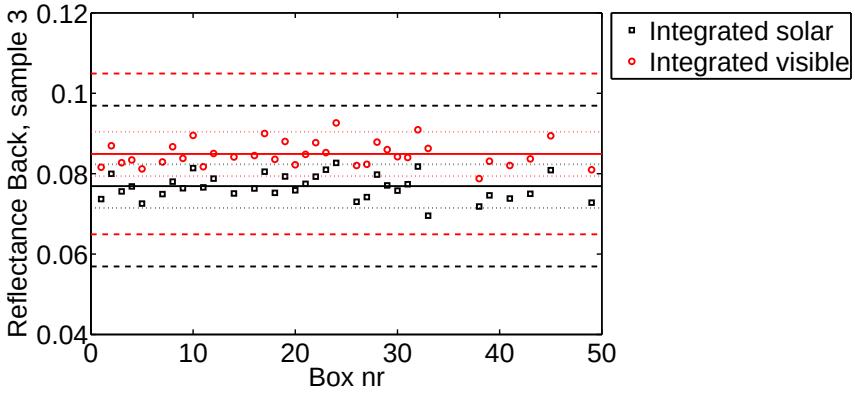
Reflectance Back, sample 3
0.12
0.1
0.08
0.06
0.04
0
10
20
30
40
50
Box nr
Integrated solar
Integrated visible

B.4 Sample #4

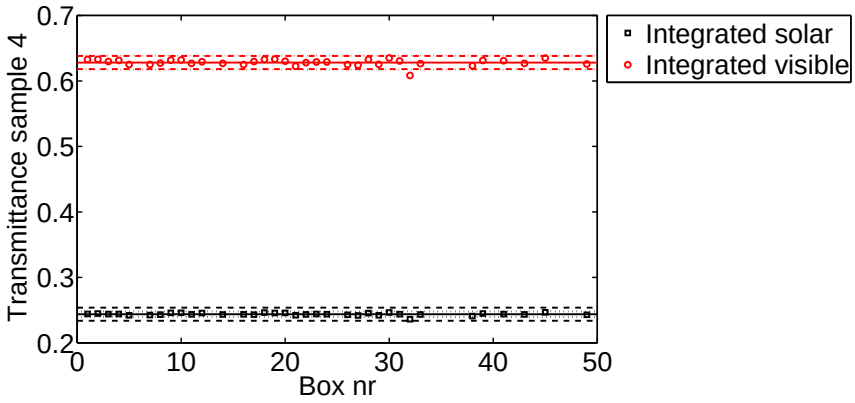
Transmittance sample 4
Box nr
Integrated solar
Integrated visible
0.7
0.6
0.5
0.4
0.3
0.2
0
10
20
30
40
50

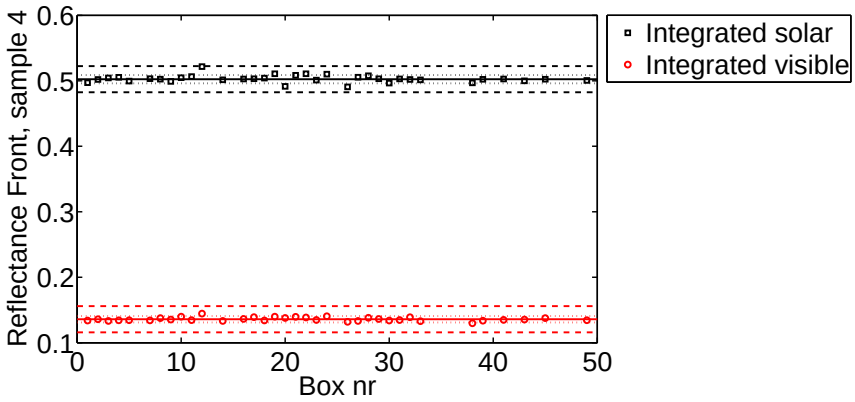
Reflectance Front, sample 4
Box nr
Integrated solar
Integrated visible
0.6
0.5
0.4
0.3
0.2
0.1
0
10
20
30
40
50

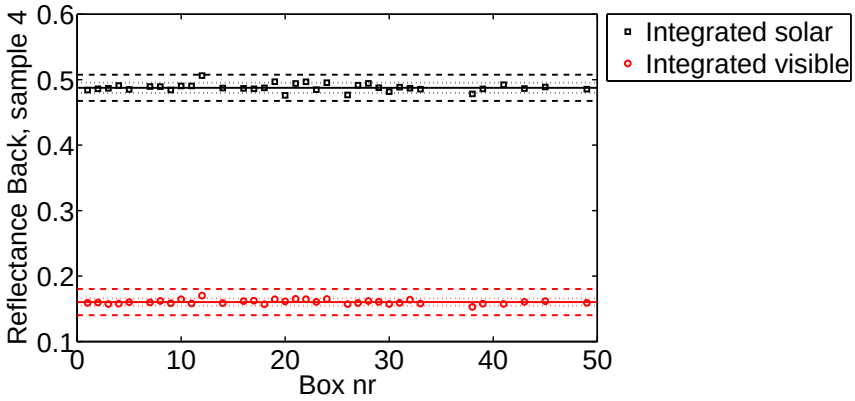
Reflectance Back, sample 4
Box nr
Integrated solar
Integrated visible
0.6
0.5
0.4
0.3
0.2
0.1
0
10
20
30
40
50

B.5 Sample #5

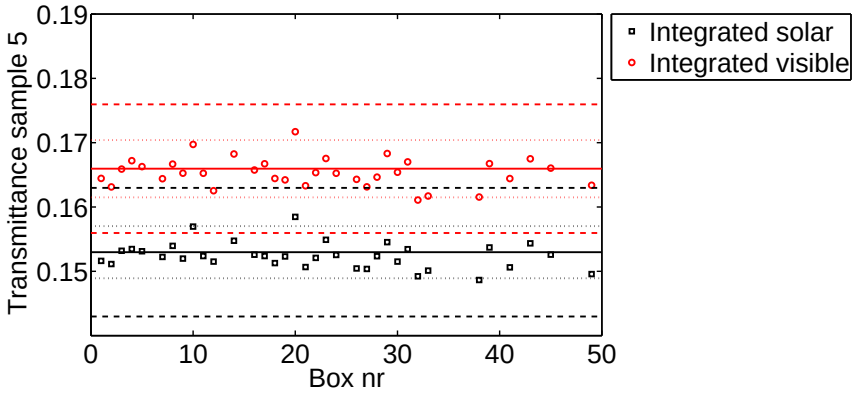
Transmittance sample 5
0.19
0.18
0.17
0.16
0.15
0
10
20
30
40
50
Box nr
Integrated solar
Integrated visible

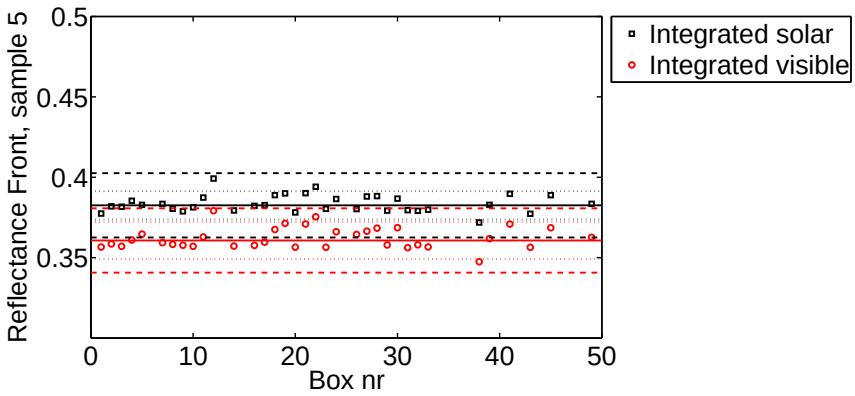
Reflectance Front, sample 5
0.5
0.45
0.4
0.35
0
10
20
30
40
50
Box nr
Integrated solar
Integrated visible

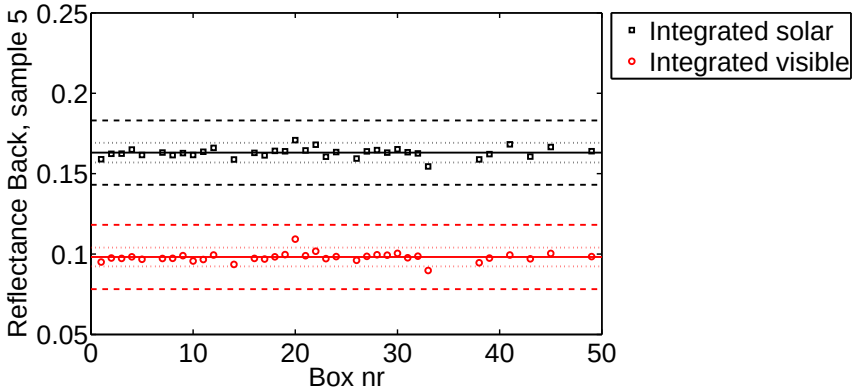
Reflectance Back, sample 5
0.25
0.2
0.15
0.1
0.05
0
10
20
30
40
50
Box nr
Integrated solar
Integrated visible

B.6 Sample #6

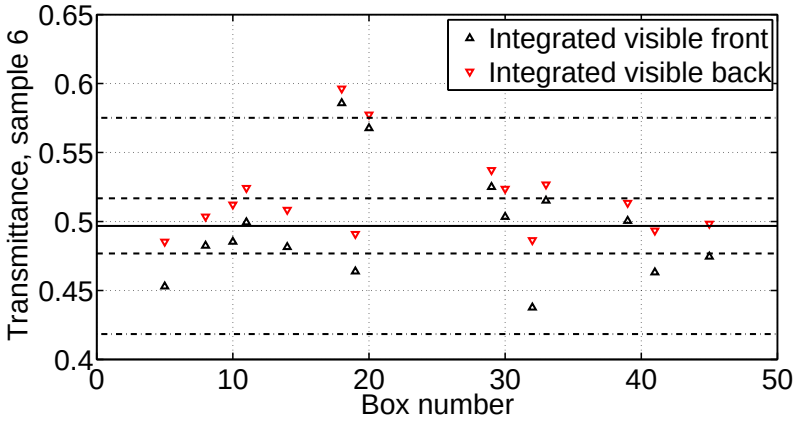
Integrated visible front
Integrated visible back
Transmittance, sample 6
Box number
0.65
0.6
0.55
0.5
0.45
0.4
0
10
20
30
40
50

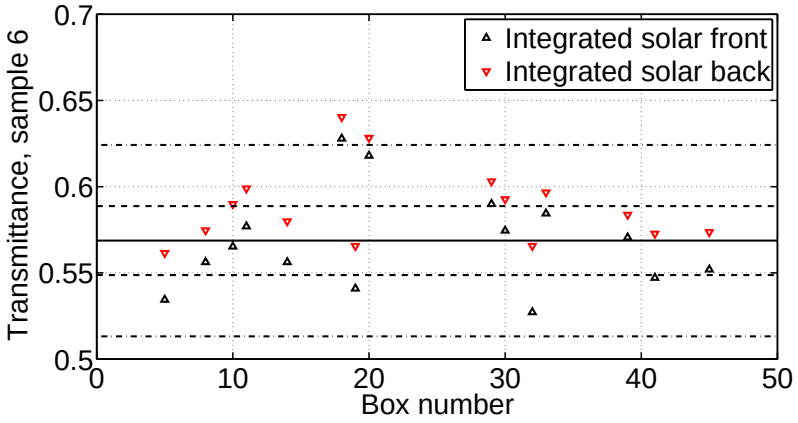
Integrated solar front
Integrated solar back
Transmittance, sample 6
Box number
0.7
0.65
0.6
0.55
0.5
0
10
20
30
40
50

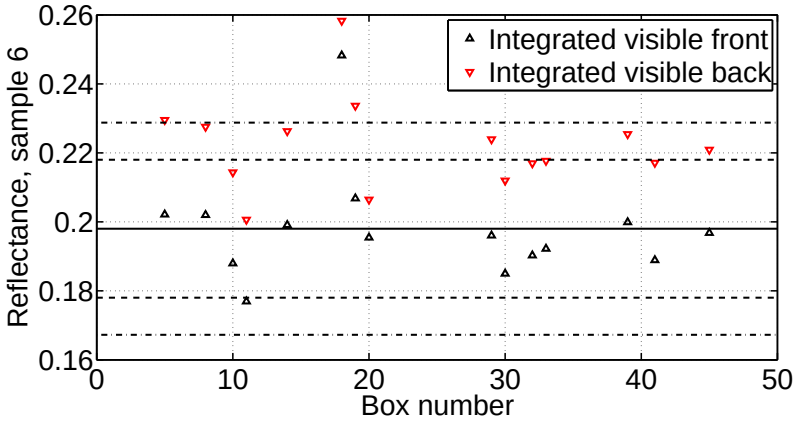
Integrated visible front
Integrated visible back
Reflectance, sample 6
Box number
0.26
0.24
0.22
0.2
0.18
0.16
0
10
20
30
40
50

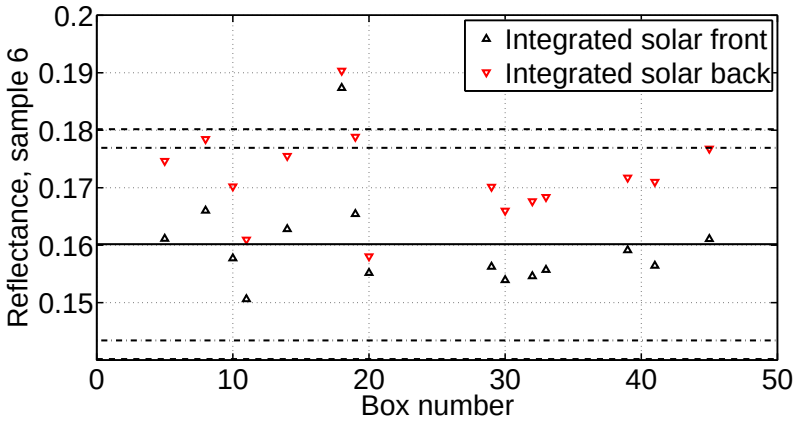
Integrated solar front
Integrated solar back
Reflectance, sample 6
Box number
0.2
0.19
0.18
0.17
0.16
0.15
0
10
20
30
40
50

B.7 Sample #7

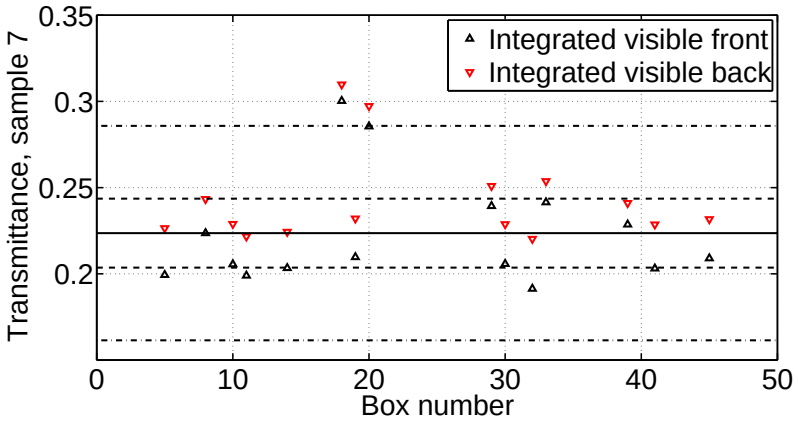
Integrated visible front
Integrated visible back
Transmittance, sample 7
Box number
0.35
0.3
0.25
0.2
0
10
20
30
40
50

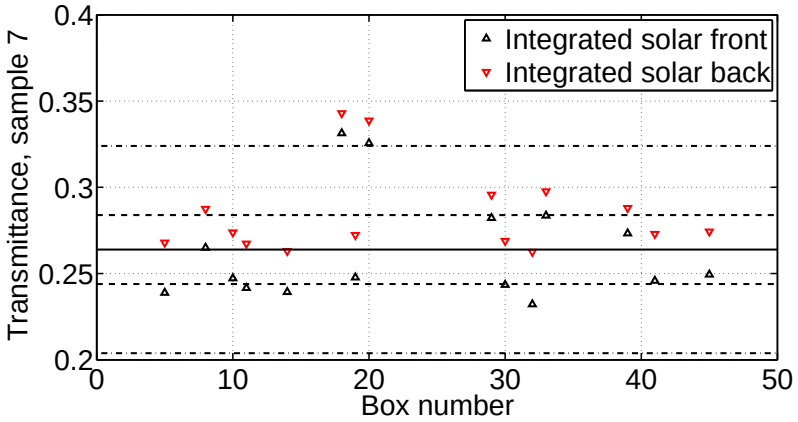
Integrated solar front
Integrated solar back
Transmittance, sample 7
Box number
0.4
0.35
0.3
0.25
0.2
0
10
20
30
40
50

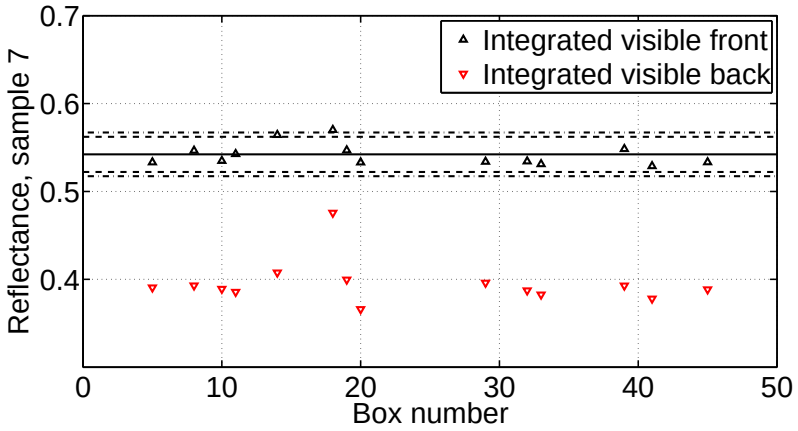
Integrated visible front
Integrated visible back
Reflectance, sample 7
Box number
0.7
0.6
0.5
0.4
0
10
20
30
40
50

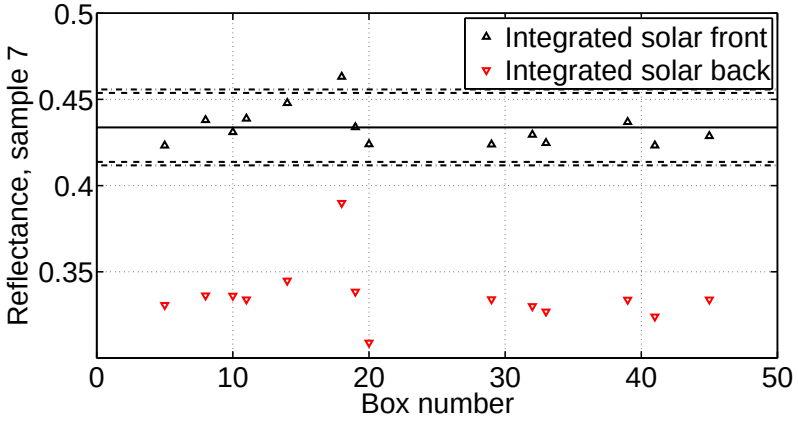
Integrated solar front
Integrated solar back
Reflectance, sample 7
Box number
0.5
0.45
0.4
0.35
0
10
20
30
40
50

B.8 Sample #8

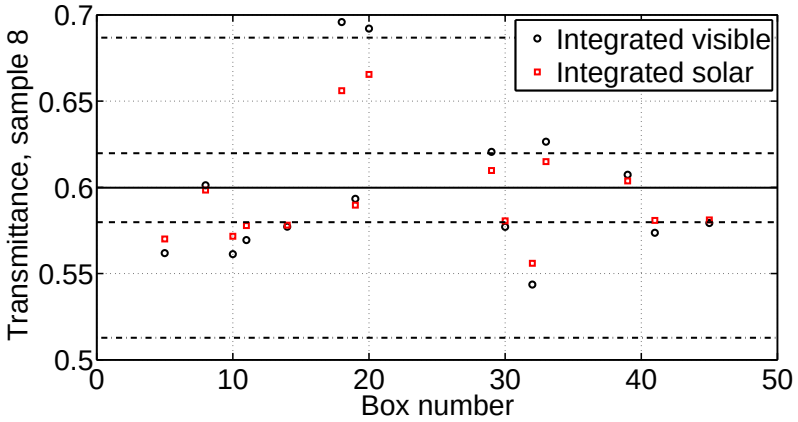
Integrated visible
Integrated solar
Transmittance, sample 8
Box number
0.7
0.65
0.6
0.55
0.5
0
10
20
30
40
50

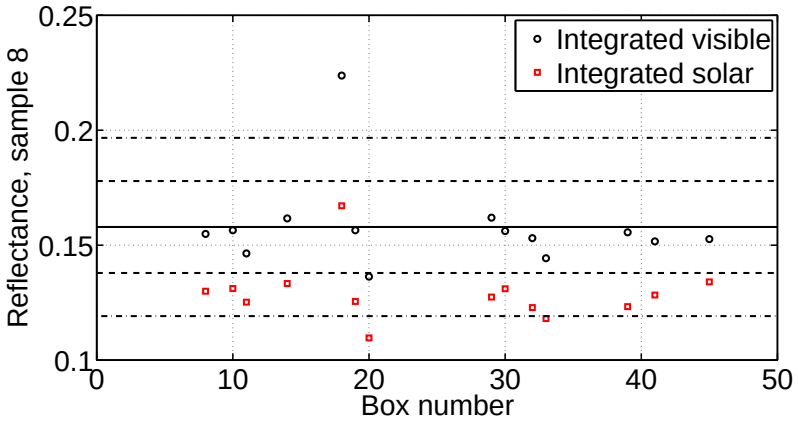
Integrated visible
Integrated solar
Reflectance, sample 8
Box number
0.25
0.2
0.15
0.1
0
10
20
30
40
50

B.9 Sample #9

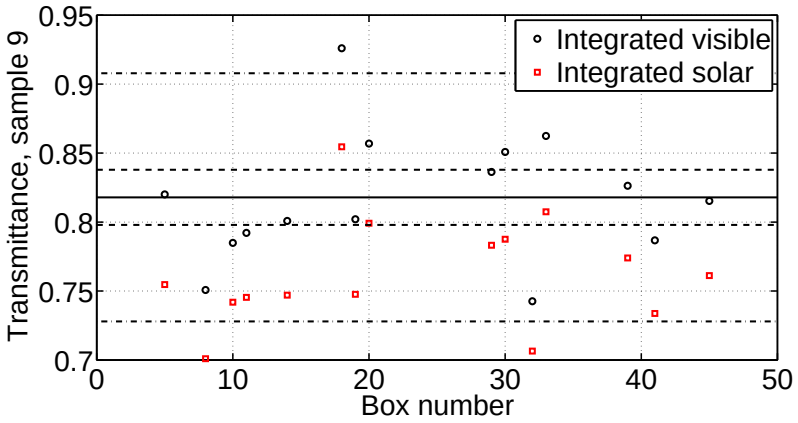
Integrated visible
Integrated solar
Transmittance, sample 9
Box number
0.95
0.9
0.85
0.8
0.75
0.7
0
10
20
30
40
50

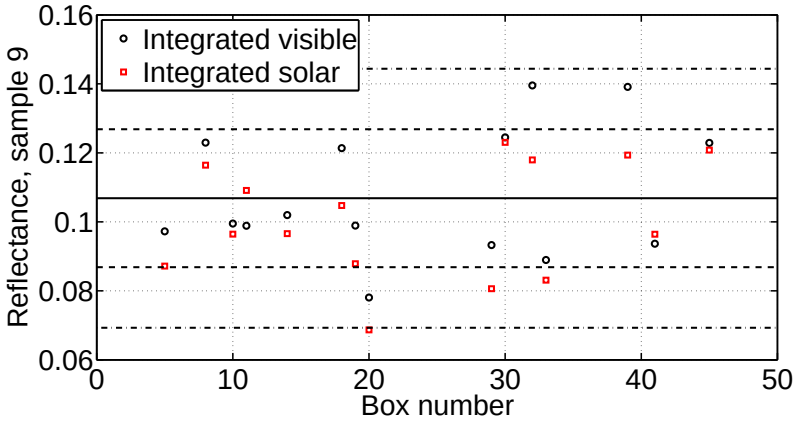
Integrated visible
Integrated solar
Reflectance, sample 9
Box number
0.16
0.14
0.12
0.1
0.08
0.06
0
10
20
30
40
50

B.10 Sample #10

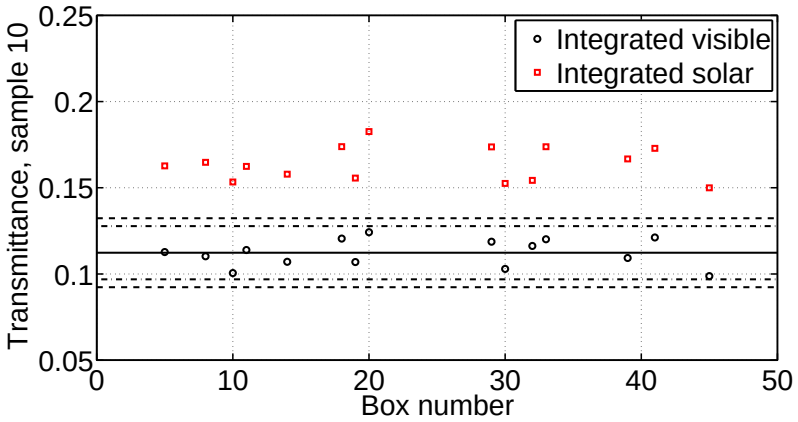

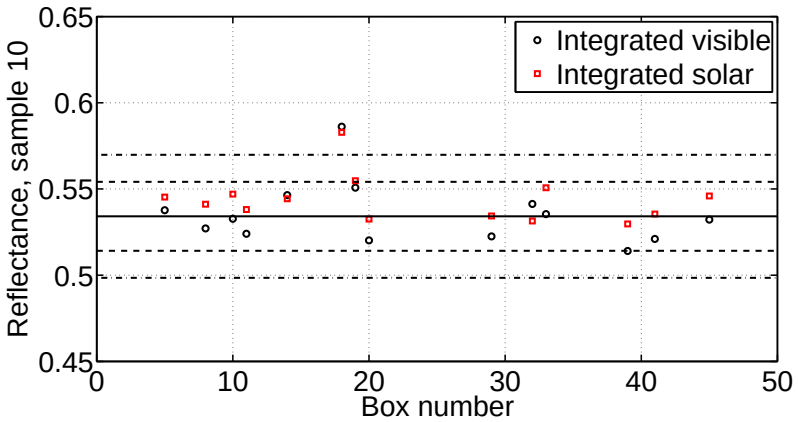

C Graphs for all IR measurements

The graphs in this section shows the calculated emissivity for the participants that submitted spectral IR data and submitted emissivity values for the participants that did not do so. The individual markers (squares and circles) show reported values, dotted lines show plus and minus two times the calculated standard deviation, and finally dashed lines show limits imposed by NFRC 302 (.02 for emissivity). The average is calculated from all values.

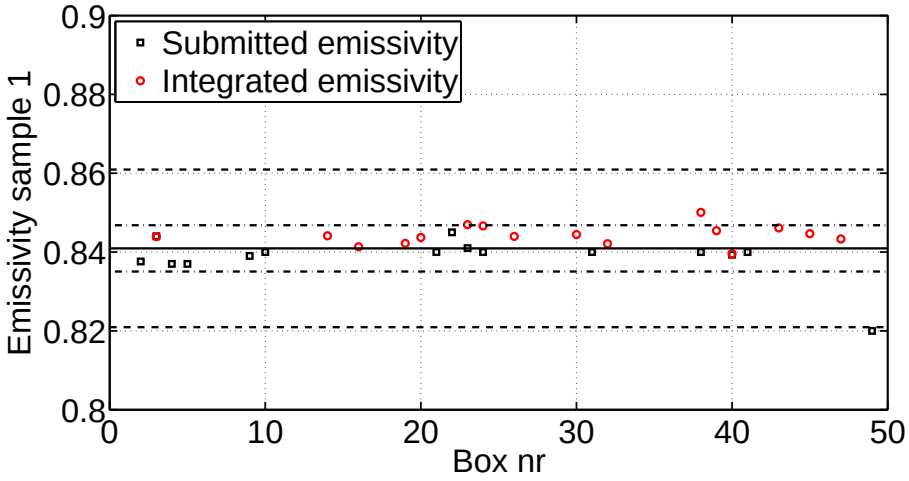

Figure 16: Calculated emissivity of uncoated glass surface of sample 1.

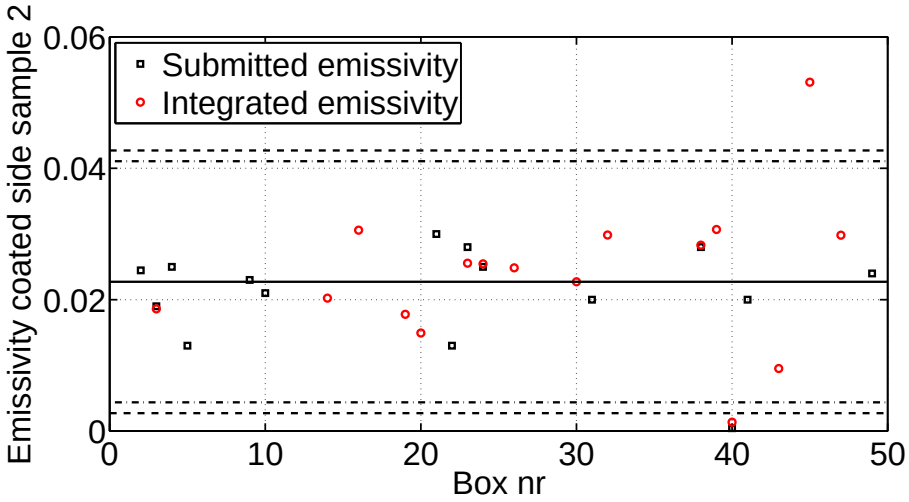

Figure 17: Calculated emissivity of coated surface of sample 2.

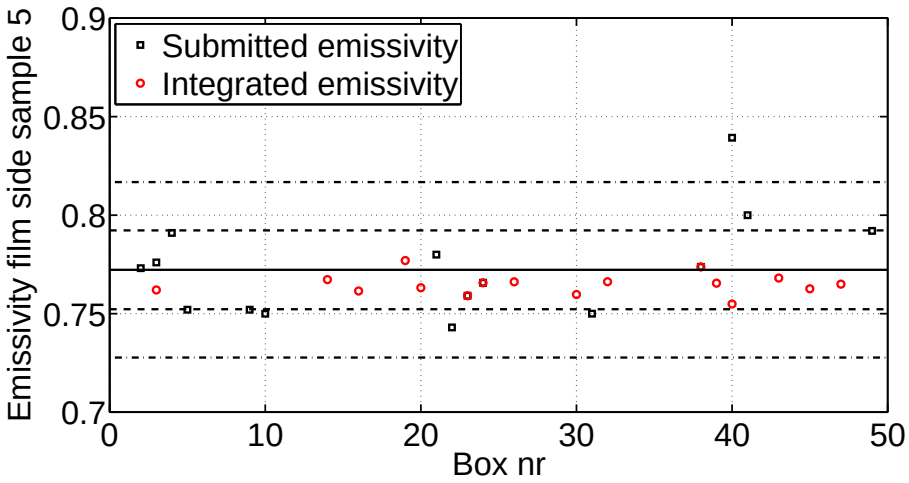

Figure 18: Calculated and submitted emissivity of film side of sample 5.

References

[1] Lawrence Berkeley National Laboratory, "IGDB – the Iinternational Glazing DataBase," 2007. http://windows.lbl.gov/materials/igdb/.

[2] National Fenestration Rating Council, "NFRC302: Verification program for optical spectral data," 2010.

[3] Lawrence Berkeley National Laboratory, "Window 6," 2009. http://windows.lbl.gov/software/window/6/index.html.

[4] D. Edwards, J. Gier, K. Nelson, and D. Roddrick, "Integrating sphere for imperfectly diffuse samples," *Appl. Opt.* **51**, pp. 1279–1288, 1961.

[5] F. J. J. Clarke and J. A. Compton, "Correction methods for integrating-sphere measurement of hemispherical reflectance," *Color Research and Application* **11**(4), pp. 253–262, 1986.

[6] W. Platzer, "Solar transmission of transparent insulation material," *Sol. Energy Mat.* **16**, pp. 275–283, 1987.

[7] A. Roos, "Interpretation of integrating sphere signal output for nonideal transmitting samples," *Applied Optics* **30**(4), pp. 468–474, 1991.

[8] A. Roos, "Use of an integrating sphere in solar energy research," *Solar Energy Materials and Solar Cells* **30**, pp. 77–94, 1993.

[9] D. Rönnow and A. Roos, "Stray-light corrections in integrating-sphere measurements on low-scattering samples," *Applied Optics* **33**(25), pp. 6092–6097, 1994.

[10] D. I. Milburn and K. G. T. Hollands, "Solar transmittance measurements using an integrationg sphere with broad area irradiation," *Solar Energy* **52**(6), pp. 497–507, 1994.

[11] D. I. Milburn and K. Hollands, "The directional response of an integrating sphere detector system," *Opt. Comm.* **115**, pp. 158–169, 1995.

[12] P. Nostell, A. Roos, and D. Rönnow, "Single-beam integrating sphere spectrphotometer for reflectance and transmittance measurements versus angle of incidence in the solar wavelength range on fiffuse and specular samples," *Rev. Sci. Instr.* **70**, pp. 2481–2494, 1999.

[13] A. V. Prokhorov, S. N. Mekhontsev, and L. M. Hanssen, "Monte carlo modeling of an integrating sphere reflectometer," *Applied Optics* **42**, pp. 3832–3842, 2003.

[14] J. C. Jonsson, A. Roos, and G. B. Smith, "Light trapping in translucent samples and its effect on the hemispherical transmittance obtained by an integrating sphere," in *Proceedings of SPIE's 48th Annual Meeting*, **5192**, pp. 91–100, 2003.

[15] G. B. Smith, J. C. Jonsson, and J. Franklin, "Spectral and global diffuse properties of high-performance translucent polymer sheets for energy efficient lighting and skylights," *Appl. Opt.* **42**(19), pp. 3981–3991, 2003.

[16] J. C. Jonsson, M. Rubin, A. M. Nilsson, A. Jonsson, and A. Roos, "Optical characterization of fritted glass for architectural applications," *Optical Materials* **31**, pp. 949–958, 2009.

[17] J. C. Jonsson and M. Rubin, "Light-loss when measuring transmittance of thick scattering samples with an integrating sphere," in *Proceedings of SPIE*, R. Winston and J. Koshel, eds., **6670**, p. 667007, 2007.

[18] L. M. Hanssen, "Effects of restricting the detector field of view when using integrating spheres," *Applied Optics* **28**, pp. 2097–2103, 2003.

[19] N. Kotey, J. L. Wright, and M. Collins, "Determining off-normal solar optical properties of drapery fabrics," in *ASHRAE Transactions*, **115**, 2009.

[20] P. Polato, G. Rossi, J. Roucour, J. Simons, and H. Rose-Wilson, "Spectrophotometric determination of visible and solar parmeters of sand-blasted glass panes and translucent glass laminates," *Riv. Staz. Sper. Vetro* **33**(5), pp. 5–18, 2003.

[21] H. Wilson, M. Hutchins, N. Kilbey, and C. Anderson, "Intercomparison of transmittance and reflectance measurements of light-scattering and patterned glass with spectrophotometers and integrating spheres," 2009. ICG TC-10.

[22] H. Wilson, J. Bretschneider, T. Hofmann, M. Hutchins, J. Jonsson, M. Kermel, I. Marenne, A. Roos, P. van Nijnatten, and T. Kuhn, "Transmissionsgrad von strukturglas für solare anwendungen - ergebnisse eines ringversuchs des ICG-TC10," in *20. OTTI-Symposium Thermische Solarenergie 2010*, pp. 355–360, 2010.

[23] H. R. Wilson, J. Bretschneider, T. Hofmann, M. Hutchins, J. Jonsson, C. Kermel, I. Marenne, A. Roos, and P. van Nijnatten, "Transmittance of patterned solar glass panes results of a measurement round robin by ICG-TC10," in *Tagungsband Colloquium Optische Spektrometrie COSP 2011, Berlin, Germany*, 2011.

[24] H. R. Wilson, J. Bretschneider, T. Hofmann, M. Hutchins, J. Jonsson, C. Kermel, I. Marenne, A. Roos, and P. van Nijnatten, "Transmittance of patterned solar glass panes results of a measurement round robin by icg-tc10," in *Conf. Proc. 11th ESG Conference, Maastricht, Netherlands*, 2012.

[25] A. M. Nilsson, A. Jonsson, J. C. Jonsson, and A. Roos, "Method for more accurate transmittance measurements of low-angle scattering samples using an integrating sphere with an entry port beam diffuser," *Applied Optics* **50**, pp. 999–1006, 2011.

[26] W. Möller, K. Nikolaus, and A. Höpe, "Degradation of the diffuse reflectance of spectralon under low-level irradiation," *Metrologia* **40**, pp. 212–215, 2003.

[27] A. S. for Testing and Materials, "ASTM D1003: Standard test method for haze and luminous transmittance of transparent plastics," 2011.

[28] A. Roos and C. G. Ribbing, "Interpretation of integrating sphere signal output for non-lambertian samples," *Applied Optics* **27**, pp. 3833–3837, 1988.

[29] N. Kotey, *Measurement and Models Related to Solar Optics in Windows with Shading Devices*. PhD thesis, University of Waterloo, 2009. http://libdspace.uwaterloo.ca/bitstream/10012/4309/3/PhD Thesis Final_Nathan Kote.pdf.

[30] "THERMES, thermal emissivity of energy-saving coatings on glass - preservation of the measuremnt infrastructure of the glazing industry," tech. rep., EU Growth Programme Contract G6RD-CT-2001-00658, 2001.

[31] K. Gelin, A. Roos, P. van Nijnatten, and F. Geotti-Bianchini, "Thermal emittance of coated glazing - simulation versus measurement," *Optical Materials* **27**, pp. 705–712, 2005.

[32] P. van Nijnatten, M. Hutchins, A. Roos, F. Geotti-Bianchini, P. Polato, C. Anderson, F. Olive, M. Köhl, R. Spragg, and P. Turner, "Thermal emissivity of energy-saving coatings on glass: The THERMES project," in *4th International Conference on Coatings on Glass*, 2002. Braunschweig, Germany.

[33] National Fenestration Rating Council, "NFRC301: Standard test method fo emittance of specular surfaces using spectrometric measurements," 2010.

[34] European Committee for Standardization, "EN673: Glass in building - determination of thermal transmittance (u value) - calculation method," 1997.

[35] M. Rubin, D. Arasteh, and J. Hartmann, "A correlation between normal and hemispherical emissivity of low-emissivity coatings on glass," *Int. Comm. Heat Mass Transfer* **14**, pp. 561–565, 1987.